

Adaptive Model Predictive Control for Real-Time Dispatch of Energy Storage Systems

David A. Copp, Tu A. Nguyen, and Raymond H. Byrne

Abstract—Energy storage systems are flexible and controllable resources that can provide a number of services for the electric power grid. Many technologies are available, and corresponding models vary greatly in level of detail and tractability. In this work, we propose an adaptive optimal control and estimation approach for real-time dispatch of energy storage systems that neither requires accurate state-of-energy measurements nor knowledge of an accurate state-of-energy model. Specifically, we formulate an online optimization problem that simultaneously solves moving horizon estimation and model predictive control problems, which results in estimates of the state-of-energy, estimates of the charging and discharging efficiencies, and future dispatch signals. We present a numerical example in which the plant is a nonlinear, time-varying Lithium-ion battery model and show that our approach effectively estimates the state-of-energy and dispatches the system without accurate knowledge of the dynamics and in the presence of significant measurement noise.

I. INTRODUCTION

Energy storage systems are flexible and controllable resources that play a key role in development of the future electric power grid. Energy storage systems can provide a number of power and energy applications that improve the reliability and resilience of power grids, from frequency regulation and voltage support, to backup power and enabling the integration of intermittent renewable generation [1]. However, there are several challenges that need to be addressed before energy storage can be widely adopted. One of these challenges is that accurate technology-specific energy storage system models are complicated and may be intractable to solve or are simply not known. Therefore, models that are used suffer from potentially large inaccuracy and uncertainty. For instance, the state-of-energy (SoE) dynamics of a battery energy storage system (BESS) are generally time-varying and nonlinear and depend on operating conditions, age, and cell balancing. Therefore, estimating the SoE of a multi-cell battery pack is challenging, and state estimates from a battery management system (BMS) can have significant error [2]. In the past, some methods have mitigated this by restricting the SoE to a small operating range so that linear SoE dynamics can be used or by using heuristic control approaches. For example, a rule-based heuristic that updates a control strategy

D. Copp, T. Nguyen, and R. Byrne are with Sandia National Laboratories, Albuquerque, NM 87185-1108 USA (e-mail: dcopp@sandia.gov). Sandia National Laboratories is a multi-mission laboratory managed and operated by National Technology and Engineering Solutions of Sandia, LLC., a wholly owned subsidiary of Honeywell International, Inc., for the U.S. Department of Energy's National Nuclear Security Administration under contract DE-NA-0003525. Funding for this research was provided by the US DOE Energy Storage Program managed by Dr. Imre Gyuk of the DOE Office of Electricity Delivery and Energy Reliability.

as a function of SoE is presented in [3]. Unfortunately, these methods are not optimal and may severely limit the capabilities of the system.

Online estimation and control have the advantage of updating state estimates and control actions whenever new feedback measurements are available and may be used to alleviate some of the challenges associated with estimation and control of a BESS. Example optimization-based approaches to estimation and control are moving horizon estimation (MHE) [4] and model predictive control (MPC) [5], [6], respectively. Both of these approaches involve the solution of a finite horizon online optimization problem at each time step and can explicitly handle system constraints. Given a finite sequence of past measurements and past control inputs, solving an MHE problem results in a current state estimate. Given an estimate of the system's current state, solving an MPC problem results in a finite sequence of future control actions and state predictions. However, both MHE and MPC rely on a model of the system, which can be inaccurate and uncertain for a BESS.

In this work, we propose an adaptive approach that combines MPC and MHE problems for the real-time dispatch of energy storage systems. This approach involves solving both MHE and MPC problems simultaneously as a single min-max optimization problem and includes uncertain model parameters as decision variables to be estimated and updated online. This output-feedback approach to MPC for constrained nonlinear systems was proposed in [7] and [8]. Several applications and examples of using this approach for adaptation and learning are given in [9]. In this work, we specialize the approach for energy storage dispatch.

Our proposed approach does not rely on accurate SoE measurements from the BMS. Instead, it computes its own state estimate based on an adaptively updated model within the energy management system (EMS). Even if the true system dynamics are not known, a simplified model of the dynamics with adaptively updated parameters may be effectively used. In fact, in a numerical example, we show that using a simple linear energy flow model with adaptively updated values for the charging and discharging efficiencies within this combined MPC/MHE approach results in effective estimation and control of a simulated nonlinear, time-varying Lithium-ion BESS.

Several adaptive approaches to MPC have been proposed, and optimal control approaches considering the modeling challenges of a BESS have been used in several power and energy applications. Adaptive MPC for constrained nonlinear systems is presented in [10]. MPC for nonlinear systems with

uncertain parameters with known probability distributions is discussed in [11]. A dual adaptive MPC approach is presented in [12] that considers uncertain linear systems and updates estimates of the unknown parameters at each sampling time. The original stochastic problem is reformulated as a quadratically-constrained quadratic-programming problem and is readily solved. Adaptive MPC using MHE for parameter estimation for constrained linear systems is presented in [13]. In [14], an adaptive switched MPC approach is proposed for dispatching energy from a system including a photovoltaic array, diesel generator, and BESS that similarly estimates the charging and discharging efficiencies of an energy flow model online, but a constant efficiency (time-invariant) linear model is used as the plant. An approximation of a first-principles electrochemical model for a Lithium-ion BESS is developed and employed in a quadratic dynamic matrix controller, which takes into account constraints on current, state-of-charge, and temperature, to minimize battery charging time in [15]. Furthermore, optimization approaches are common in techno-economic analyses of energy storage systems. An MPC approach for maximizing revenue of a BESS and wind energy conversion system participating in energy markets with additional constraints on depth-of-discharge and daily number of cycles to expand the lifetime of the BESS is presented in [16]. A dynamic programming approach is used to solve the offline optimization of maximizing potential revenue from a BESS with nonlinear, technology-specific models in [17].

The rest of the paper is organized as follows. The problem formulation and modeling of energy storage systems are discussed in Section II. Our proposed adaptive approach for real-time dispatch is presented in Section III. A numerical example is given in Section IV, and conclusions and future work are discussed in Section V.

II. PROBLEM FORMULATION

We consider the problem of optimally dispatching a grid-connected BESS in real-time. The dispatch signals are usually computed by an EMS that communicates with the BESS. The architecture of a BESS connected to an EMS and the grid is shown in Figure 1. The components of a BESS are the battery (BAT), the power conversion system (PCS), which interfaces the BESS with the grid, the PCS controller, which performs the primary control function of tracking a power reference, and the BMS, which monitors the system and individual cells by taking measurements, such as voltage, current, and temperature, and calculates estimates of the BESS states. The solid black lines between the grid, PCS, and BAT in Figure 1 indicate the path along which power flows. It is within those connections where losses that depend on the BESS state and current operating conditions occur.

The EMS performs higher-level computations and determines dispatch signals for the BESS that depend on the application for which the BESS is being used. The inputs to the EMS are the outputs of the BMS (often estimates of the BESS SoE, voltage, current, temperature, and other quantities) and data from the grid (such as energy prices or system

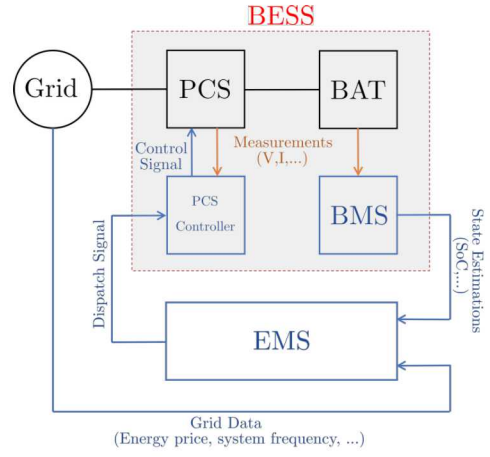


Fig. 1. Grid-connected BESS and EMS architecture.

states, like frequency) that are necessary to determine the best dispatch signal for a particular application. Computing effective real-time dispatch signals can be a challenge due to significant noise in the measurement signals and potentially inaccurate and uncertain models within the EMS. Therefore, we would like to design EMS control algorithms that are robust to these types of errors and uncertainties.

A. Modeling Energy Storage Systems

Models for energy storage systems vary in their level of detail and are often technology-specific. In this section, we briefly discuss energy flow models of energy storage systems that may be used in a BMS or EMS.

1) *Nonlinear Energy Flow Model*: A general discrete-time nonlinear energy flow model can be used to describe the SoE dynamics of a BESS and is given as

$$x_{t+1} = x_t + f_t^c(x_t, u_t^c)\tau - f_t^d(x_t, u_t^d)\tau, \quad (1)$$

where $x_t \in \mathbb{R}_{\geq 0}$ is the SoE (in units of energy) at time $t \in \mathbb{Z}_{\geq 0}$, $u_t = [u_t^c \ u_t^d]^\top \in \mathbb{R}_{\geq 0}^2$ is the vector of dispatch signals (charge and discharge power commands $u_t^c \in \mathbb{R}_{\geq 0}$ and $u_t^d \in \mathbb{R}_{\geq 0}$, respectively) at time t , $\tau \in \mathbb{R}_{>0}$ denotes the duration of each discrete time step, and $f_t^c : \mathbb{R}^2 \rightarrow \mathbb{R}$ and $f_t^d : \mathbb{R}^2 \rightarrow \mathbb{R}$ are generally nonlinear time-varying functions that depend on the energy storage technology considered. As a representative example, we next present the functions f_t^c and f_t^d for a Lithium-ion battery system that depend on battery cell parameters, the charge and discharge power commands, and the SoE of the BESS. This Lithium-ion BESS model is described in, e.g., [17], and is derived from the Tremblay-Dessaint model [18].

Lithium-ion Battery:

$$f_t^c(x_t, u_t^c) = \eta_{\text{pcs}} u_t^c - p_t^{lc}, \quad (2a)$$

$$f_t^d(x_t, u_t^d) = \frac{1}{\eta_{\text{pcs}}} u_t^d + p_t^{ld}, \quad (2b)$$

where $\eta_{\text{pcs}} \in (0, 1)$ denotes the efficiency of the PCS, and $p_t^{lc} \in \mathbb{R}_{\geq 0}$ and $p_t^{ld} \in \mathbb{R}_{\geq 0}$ are the power losses of the

BESS during charge and discharge, respectively, and can be approximated as

$$p_t^{lc} = \frac{Q}{V\bar{x}} \left[\left(R + \frac{C\bar{x}}{\bar{x} - x_t} \right) (\eta_{\text{pcs}} u_t^c)^2 + \frac{C\bar{x}(\bar{x} - x_t)}{x_t} (\eta_{\text{pcs}} u_t^c) \right],$$

$$p_t^{ld} = \frac{Q}{V\bar{x}} \left[\left(R + \frac{C\bar{x}}{x_t} \right) \left(\frac{u_t^d}{\eta_{\text{pcs}}} \right)^2 + \frac{C\bar{x}(\bar{x} - x_t)}{x_t} \left(\frac{u_t^d}{\eta_{\text{pcs}}} \right) \right],$$

where $\bar{x} \in \mathbb{R}_{>0}$ is the energy capacity of the BESS (in units of energy), $Q \in \mathbb{R}_{>0}$ is the rated capacity of a battery cell in Ah, $V \in \mathbb{R}_{>0}$ is the rated DC voltage of a battery cell in Volts, $R \in \mathbb{R}_{>0}$ is the internal resistance of a battery cell in Ohms, and $C \in \mathbb{R}_{>0}$ is a model coefficient that can be calculated from the nameplate or testing data of a battery cell.

2) *Linear Energy Flow Model*: Similarly, a linear energy flow model may be used for the SoE dynamics of a BESS and is given as the following discrete linear time-invariant model

$$x_{t+1} = x_t + \eta_c u_t^c \tau - \frac{1}{\eta_d} u_t^d \tau, \quad (4)$$

where $\eta_c \in (0, 1)$ denotes the BESS charging efficiency and $\eta_d \in (0, 1)$ denotes the BESS discharging efficiency. Many existing EMS control algorithms utilize a linear energy flow model even though it does not accurately describe the SoE dynamics, especially as operating conditions change with time. To account for model uncertainty or noise, we can write the output of the linear energy flow model (4) as

$$y_t = x_t + n_t, \quad (5)$$

where $n_t \in \mathbb{R}$ is noise on measurement $y_t \in \mathbb{R}$ at time t .

III. ENERGY STORAGE DISPATCH

In this section, we present methods that can be implemented in an EMS for real-time dispatch of energy storage systems.

A. Nonlinear Model Predictive Control Approach

We first present a nonlinear MPC approach for real-time dispatch of an energy storage system. Given an estimate of the current SoE, this approach involves solving a finite-horizon online optimization problem at every time t , which results in a sequence of dispatch signals to be applied and associated SoE predictions. First we define some notation: The set $\mathcal{T} := \{t, t+1, \dots, t+T-1\}$ is the set of discrete times in the finite forward time horizon considered. T is length of the time horizon. Given a discrete-time signal $z : \mathbb{Z}_{\geq 0} \rightarrow \mathbb{R}^n$ and two times t_1, t_2 with $t_1 < t_2$, we denote by $z_{t_1:t_2}$ the sequence $\{z_{t_1}, z_{t_1+1}, \dots, z_{t_2}\}$.

With this notation, we can write the optimization problem that we would like to solve as

$$\min_{\hat{u}_{t:t+T-1}} \sum_{k=t}^{t+T-1} J_k^{\text{MPC}}(\hat{x}_k, \hat{u}_k) \quad (6)$$

subject to the following constraints for all $k \in \mathcal{T}$:

$$\hat{x}_t = x_0 \quad (7a)$$

$$\|\hat{u}_k\|_\infty \leq \bar{u} \quad (7b)$$

$$\alpha\bar{x} \leq \hat{x}_k + f_k^c(\hat{x}_k, \hat{u}_k^c)\tau - f_k^d(\hat{x}_k, \hat{u}_k^d)\tau \leq (1 - \beta)\bar{x} \quad (7c)$$

The objective function $J_k^{\text{MPC}} : \mathbb{R} \times \mathbb{R}^2 \rightarrow \mathbb{R}$ encodes the application in which the energy storage system is participating and depends on the dispatch signals \hat{u}_k and the SoE predictions \hat{x}_k . Constraint (7a) ensures that the initial state is equal to the given estimate x_0 . Constraint (7b) ensures that the charged and discharged power from the BESS is less than or equal to the power rating \bar{u} . Constraint (7c) ensures that the predicted SoE \hat{x}_k (computed using model (1) with \hat{u}_k) is greater than or equal to, and less than or equal to, a desired fraction of the energy capacity \bar{x} . The scalars $\alpha, \beta \in [0, 1]$ are the desired fractions of unused SoE at the lower and upper limits of the BESS energy capacity, respectively. These parameters are often chosen to limit the depth of charge and discharge to, e.g., improve the cycle life of the BESS, to limit the SoE to values for which linear SoE dynamics are valid, or to ensure availability of energy from the BESS for other applications.

We denote the sequence that minimizes (6) at time t as $\hat{u}_{t:t+T-1}^*$ and the associated SoE predictions as $\hat{x}_{t+1:t+T}^*$. Then, at each time t , we solve (6) and use as the control input the first element of the sequence $\hat{u}_{t:t+T-1}^*$, leading to the following control law:

$$u_t = \hat{u}_t^* \quad (8)$$

The performance of this approach depends greatly on the accuracy of the SoE estimate \hat{x}_t and the accuracy of the prediction model used in constraint (7c). In practice, an accurate nonlinear model of the BESS may not be known, or even if an accurate nonlinear model is known, the resulting nonlinear optimization problem may be intractable. Furthermore, it is not uncommon for the SoE measurement from the BMS to have significant error. Therefore, to compute the best dispatch signals, the EMS may require a better estimate of the SoE than the output of the BMS and would need a model that facilitates solving the optimization problem while remaining fairly accurate as the operating conditions of the system change over time. This motivates the need for an optimal control approach that is robust to measurement noise and parameter uncertainty. We present such an approach in the next subsection.

B. Adaptive Model Predictive Control Approach

In this section, we propose an adaptive estimation and control approach that can accommodate measurement noise and parameter uncertainty. In particular, we propose a combined MPC with MHE approach that, at each time step, involves the solution of a min-max optimization problem and results in state estimates, model parameter estimates, and future dispatch signals. In this approach, a predictive model, such as the linear energy flow model (4)-(5) can be used, and

the charging efficiency η_c and discharging efficiency η_d are uncertain parameters to be estimated and adaptively updated.

Since this problem involves state estimation and control computation, the objective function now contains two terms: one term involving the past data from time $t - L$ to time t , and the other involving the future control actions and state predictions from time t to time $t + T$. Therefore, the two terms can be given as

$$J^n(\hat{x}_{t-L}, u_{t-L:t-1}, y_{t-L:t}, \hat{\eta}_c, \hat{\eta}_d)$$

and

$$J^u(\hat{x}_{t+1:t+T}, \hat{u}_{t:t+T-1}, \hat{\eta}_c, \hat{\eta}_d).$$

Let us define further notation: The finite backward time horizon is comprised of the discrete times in the set $\mathcal{L} := \{t - L, t - L + 1, \dots, t - 1\}$ and has length L . The sequence of past measurements is denoted $\mathbf{y} := y_{t-L:t}$. The sequence of known past dispatch signals is denoted $\mathbf{u} := u_{t-L:t-1}$. The future control inputs to be chosen are denoted as $\hat{\mathbf{u}} := \hat{u}_{t:t+T-1}$. The estimate of the initial state is denoted as $\hat{\mathbf{x}} := \hat{x}_{t-L}$. Finally, the associated state predictions are denoted as $\tilde{\mathbf{x}} := \hat{x}_{t+1:t+T}$.

With this notation, we can write the objective function at each time step as

$$\begin{aligned} J(\hat{\mathbf{x}}, \tilde{\mathbf{x}}, \mathbf{u}, \hat{\mathbf{u}}, \mathbf{y}, \hat{\eta}_c, \hat{\eta}_d) := \\ J^u(\tilde{\mathbf{x}}, \hat{\mathbf{u}}, \hat{\eta}_c, \hat{\eta}_d) - J^n(\hat{\mathbf{x}}, \mathbf{u}, \mathbf{y}, \hat{\eta}_c, \hat{\eta}_d), \end{aligned}$$

and the optimization problem that we would like to solve as

$$\min_{\hat{\mathbf{u}}} \max_{\hat{\eta}_c, \hat{\eta}_d, \hat{\mathbf{x}}} J(\hat{\mathbf{x}}, \tilde{\mathbf{x}}, \mathbf{u}, \hat{\mathbf{u}}, \mathbf{y}, \hat{\eta}_c, \hat{\eta}_d), \quad (9)$$

subject to constraint (7b) and the following constraints:

$$0 \leq \hat{x}_k + \hat{\eta}_c \hat{u}_k^c \tau - \frac{1}{\hat{\eta}_d} \hat{u}_k^d \tau \leq \bar{x} \quad \forall k \in \mathcal{L} \quad (10a)$$

$$\alpha \bar{x} \leq \hat{x}_k + \hat{\eta}_c \hat{u}_k^c \tau - \frac{1}{\hat{\eta}_d} \hat{u}_k^d \tau \leq (1 - \beta) \bar{x} \quad \forall k \in \mathcal{T} \quad (10b)$$

$$\hat{x}_k = y_k - \hat{n}_k \quad \forall k \in \mathcal{L} \cup t \quad (10c)$$

$$\eta_c^{\min} \leq \hat{\eta}_c \leq \eta_c^{\max} \quad (10d)$$

$$\eta_d^{\min} \leq \hat{\eta}_d \leq \eta_d^{\max} \quad (10e)$$

Again, the objective function encodes the energy storage application, but it now depends on the past sequences of dispatch signals \mathbf{u} and SoE measurements \mathbf{y} , the unknown initial state $\hat{\mathbf{x}}$, the sequence of future dispatch signals to be chosen $\hat{\mathbf{u}}$, and the unknown charge efficiency $\hat{\eta}_c$ and discharge efficiency $\hat{\eta}_d$.

Constraints (10a) and (10b) replace the constraint (7c), where the nonlinear SoE dynamics are replaced with the linear energy flow dynamics, and there are separate constraints for the forward and backward horizons. Constraint (10a) is used when estimating the SoE and allows the estimate to be between zero and the energy capacity \bar{x} . Constraint (10b) is used for determining the future dispatch signals and requires that the predicted SoE values be within the same desired interval as in constraint (7c). Constraint (10c) ensures that the output dynamics (5) are satisfied. Constraints (10d) and (10e)

bound the values that $\hat{\eta}_c$ and $\hat{\eta}_d$ can take, respectively, and these bounds $\eta_c^{\min}, \eta_c^{\max}, \eta_d^{\min}$, and η_d^{\max} can be chosen using knowledge of the BESS technology and other characteristics.

This approach is robust to measurement noise and modeling error due to the maximization with respect to the uncertain efficiencies $\hat{\eta}_c$ and $\hat{\eta}_d$ and the unknown initial state \hat{x}_{t-L} . Therefore, the solutions $\hat{\eta}_c^*, \hat{\eta}_d^*$, and \hat{x}_{t-L}^* that maximize (9) can be thought of as worst-case estimates of these variables. With a slight abuse of notation, we also denote the sequence of future dispatch signals that minimizes (9) as $\hat{u}_{t:t+T-1}^*$ and the resulting SoE predictions as $\hat{x}_{t+1:t+T}^*$. We solve this optimization problem at every time t in a receding horizon fashion, leading to the same control law (8).

IV. NUMERICAL EXAMPLE

In this section, we consider the problem of dispatching an energy storage system to perform arbitrage in an energy market. In particular, we consider a Lithium-ion battery with parameters given in Table I. We consider the Lithium-ion BESS model (1)-(2) to be the plant of the system, and we use the linear energy flow model (4) as the prediction model within the adaptive MPC/MHE algorithm.

The objective is to minimize the cost of purchasing energy in the energy market while effectively estimating the SoE and the time-varying charge and discharge efficiencies at each time t . This is equivalent to maximizing the revenue received from buying and selling energy in the energy market by charging and discharging the energy storage system. Then the optimization problem we would like to solve is

$$\min_{\hat{\mathbf{u}}} \max_{\hat{\eta}_c, \hat{\eta}_d, \hat{\mathbf{x}}} \left(\sum_{k=t}^{t+T-1} \lambda_k (\hat{u}_k^c - \hat{u}_k^d) \tau - \sum_{k=t-L}^t w \hat{n}_k \right) \quad (11)$$

subject to the constraints in (7b) and (10). The parameter λ_k is the real-time locational marginal price (RTLMP) at time step k , and w is a non-negative scalar weight used to penalize unlikely values for the noise.

Next we present results from using the adaptive MPC/MHE approach and solving (11) over a week. We compare these results to results from assuming constant charge and discharge efficiencies in the linear energy flow model (4) used for prediction, i.e., solving (11) with a fixed η_c and η_d . The optimization parameters that were used are given in Table II. The real-time energy prices are the 5-minute RTLMPs from the East Cambridge node in ISO New England for January 18-24, 2018, which are available online [19]. For a fair comparison, the same measurement noise sequence was applied in each case and was generated as a sequence of normally distributed random variables with zero mean and a standard deviation of 10 kWh (2% of the energy capacity \bar{x}). Finally, these optimization problems were formulated and solved using TensCalc [20], a MATLAB toolbox for nonlinear optimization using symbolic tensor calculus, with the primal-dual algorithm described in [7].

Table III presents the results for multiple cases. The first column describes the case considered: adaptive MPC/MHE,

TABLE I
LITHIUM-ION BATTERY CELL AND BESS PARAMETERS

Parameter	Description	Value	Units
R	internal cell resistance	0.02	Ohm
C	calculated cell parameter	0.005	-
V	rated cell DC voltage	3.6	Volt
Q	rated cell capacity	2.5	Ah
\bar{x}	BESS energy capacity	500	kWh
\bar{u}	BESS power rating	250	kW
η_{pcs}	PCS efficiency	0.95	-

TABLE II
OPTIMIZATION PARAMETERS

Parameter	Description	Value	Units
τ	Time-step	1/12	hours
λ_t	Real-time LMP at time t	-	\$/kWh
T	Forward time horizon	144	-
L	Backward time horizon	36	-
w	Weight on measurement noise	10	-
η_c^{\min}	Minimum value of $\hat{\eta}_c$	0.85	-
η_c^{\max}	Maximum value of $\hat{\eta}_c$	0.98	-
η_d^{\min}	Minimum value of $\hat{\eta}_d$	0.85	-
η_d^{\max}	Maximum value of $\hat{\eta}_d$	0.98	-
α	Fraction of unused SoE	0.05	-
β	Fraction of unused SoE	0.05	-

or MPC/MHE with constant charge and discharge efficiencies. The chosen constant efficiencies (90%, 91%, 92%, and 93%) correspond to roundtrip efficiencies (i.e., $\eta_c \eta_d$) of 81% to 86.5%. Column two presents the generated revenue from each case (calculated as $-\sum_t \lambda_t (u_t^c - u_t^d) \tau$, where t goes from time 00:00 on January 18 to time 23:55 on January 24, in increments of $\tau = 5$ minutes). Column three gives the root-mean-square error (RMSE) of the SoE estimate over the entire week, and column four gives values for a metric that quantifies how much constraint (10b) is violated in each case over the week. We define this constraint violation metric as

$$\epsilon = \|\dot{x} - (1 - \beta)\bar{x}\mathbf{1}\|_2 + \|\dot{x} - \alpha\bar{x}\mathbf{1}\|_2, \quad (12)$$

where \dot{x} is the vector of all x_t such that $x_t > (1 - \beta)\bar{x}$, \check{x} is the vector of all x_t such that $x_t < \alpha\bar{x}$, and $\mathbf{1}$ is a vector of appropriate length whose elements all equal one.

While the revenues generated in each case are similar, the adaptive MPC/MHE approach results in significantly lower state estimation error and smaller constraint violation metric ϵ . More accurate SoE estimation and minimal constraint violation are ideal in general but may be especially important when considering applications in which bidding of power or energy quantities is required, such as when participating in frequency regulation, or in resilience applications when a particular quantity of energy is required. In addition, other values for the constant efficiencies were considered, with $\eta_c = \eta_d$ below 0.90 or above 0.93, but resulted in dispatch signals u_t that violate the constraint (10a), i.e., the solution was physically infeasible. This is not surprising as choosing a constant efficiency too high or too low will result in overly optimistic or pessimistic, respectively, SoE predictions. Moreover, it is not surprising that the revenue for the constant efficiency cases may be slightly higher because a larger range of SoE values were (unintentionally) used (i.e.,

TABLE III
RESULTS FOR MULTIPLE CASES FOR THE WEEK OF JAN. 18-24, 2018.

Case	Revenue	RMSE of \hat{x}	Constraint violation ϵ
Adaptive	\$439.30	3.63	36.87
$\eta_c = \eta_d = 0.90$	\$437.78	13.44	168.14
$\eta_c = \eta_d = 0.91$	\$441.73	11.36	150.92
$\eta_c = \eta_d = 0.92$	\$443.49	6.52	101.34
$\eta_c = \eta_d = 0.93$	\$442.85	5.96	130.50

larger constraint violation ϵ).

Figure 2 shows the results for the entire week. It can be seen that when the RTLMP is high, the BESS discharges (sells energy in the energy market), and when the RTLMP is low, the BESS charges (buys energy in the energy market). Figure 3 shows the results for a portion of the week. It can be seen that the SoE estimate from the adaptive MPC/MHE approach closely tracks the true SoE even in the presence of significant measurement noise.

V. CONCLUSION AND FUTURE WORK

We presented an adaptive optimal control approach for dispatching energy storage systems that involved simultaneously solving a moving horizon estimation problem and a model predictive control problem. This approach estimates the state-of-energy of the energy storage system, estimates and adaptively updates the charge and discharge efficiencies, and computes resulting optimal charge and discharge dispatch signals. An accurate technology-specific model of the energy storage system is not required; in fact, only a linear energy flow model and knowledge of the system's power rating and energy capacity were required. The numerical example considered a nonlinear Lithium-ion battery system and showed that our approach, using a linear energy flow model for prediction whose efficiencies were estimated and updated online, resulted in significantly lower state-of-energy estimation error and higher constraint satisfaction when compared to the same approach assuming constant charge and discharge efficiencies.

In future work, we will implement this approach within an energy management system to dispatch a real energy storage system for which an accurate nonlinear state-of-energy model is not known. Furthermore, we will investigate optimization problem formulations for other real-time energy storage applications, such as frequency regulation, and also consider a system operation or degradation cost.

REFERENCES

- [1] R. H. Byrne, T. A. Nguyen, D. A. Copp, B. R. Chalamala, and I. Gyuk, "Energy management and optimization methods for grid energy storage systems," *IEEE Access*, vol. 6, pp. 13 231–13 260, 2018.
- [2] R. Xiong, J. Cao, Q. Yu, H. He, and F. Sun, "Critical review on the battery state of charge estimation methods for electric vehicles," *IEEE Access*, vol. 6, pp. 1832–1843, 2018.
- [3] Z. Jiang, L. Gao, and R. A. Dougal, "Adaptive control strategy for active power sharing in hybrid fuel cell/battery power sources," *IEEE Transactions on Energy Conversion*, vol. 22, no. 2, pp. 507–515, 2007.
- [4] C. V. Rao, J. B. Rawlings, and D. Q. Mayne, "Constrained state estimation for nonlinear discrete-time systems: Stability and moving horizon approximations," *IEEE Transactions on Automatic Control*, vol. 48, no. 2, pp. 246–258, 2003.

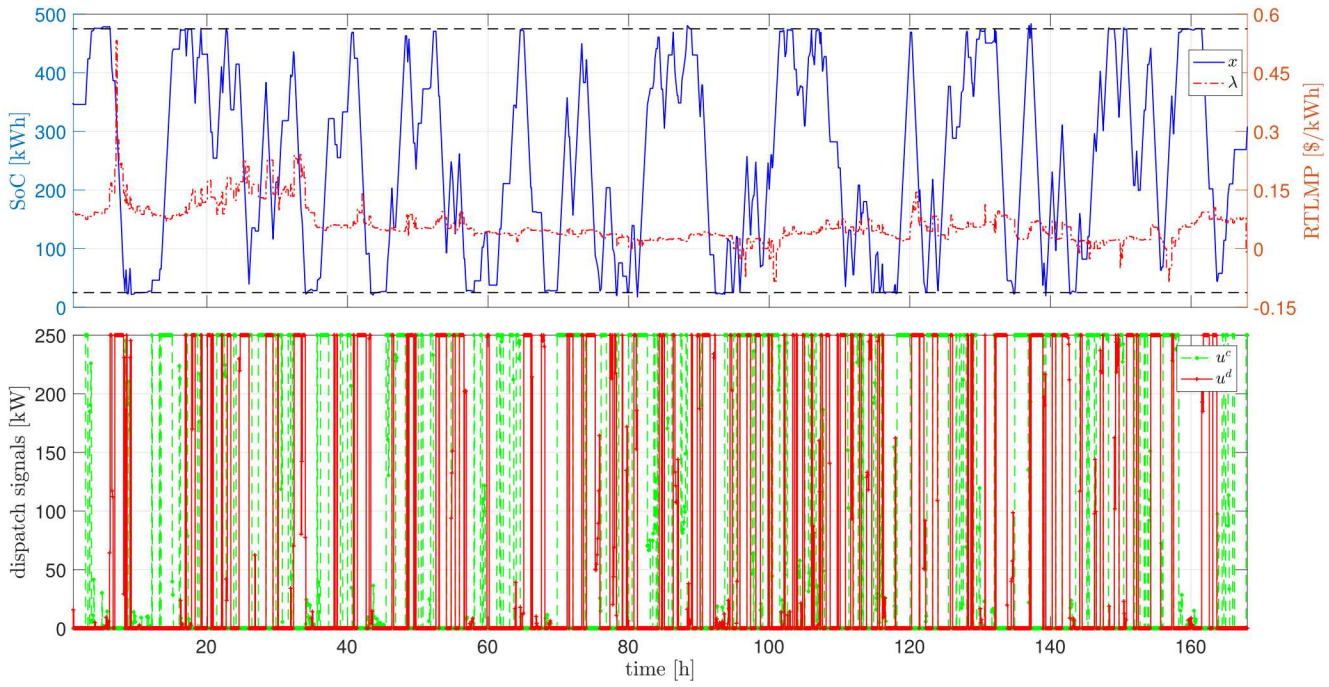


Fig. 2. Results for the week of January 18-24, 2018 using the adaptive MPC/MHE approach. The top subplot shows the values of the true SoE, x , the RTLMP, λ , and the values of $\alpha\bar{x}$ and $(1 - \beta\bar{x})$ from constraint (10b) are shown as dashed black lines. The bottom subplot shows the implemented charge and discharge dispatch signals, u^c and u^d , respectively, computed by solving (11) at each time step.

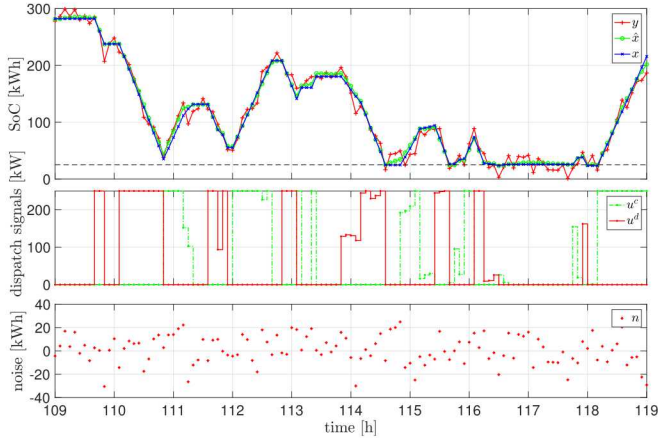


Fig. 3. Results for a portion of the week of January 18-24, 2018 using the adaptive MPC/MHE approach. The top subplot shows the SoE measurements y , SoE estimates \hat{x} , and true SoE values x . The middle subplot shows the implemented charge and discharge dispatch signals u^c and u^d , respectively. The bottom subplot shows the values of the measurement noise n .

- [5] J. B. Rawlings and D. Q. Mayne, *Model predictive control: Theory and design*. Nob Hill Pub. Madison, Wisconsin, 2009.
- [6] D. Q. Mayne, “Model predictive control: Recent developments and future promise,” *Automatica*, vol. 50, no. 12, pp. 2967–2986, 2014.
- [7] D. A. Copp and J. P. Hespanha, “Simultaneous nonlinear model predictive control and state estimation,” *Automatica*, vol. 77, pp. 143–154, 2017.
- [8] ———, “Nonlinear output-feedback model predictive control with moving horizon estimation,” in *Decision and Control (CDC), 2014 IEEE 53rd Annual Conference on*. IEEE, 2014, pp. 3511–3517.
- [9] ———, “Addressing adaptation and learning in the context of model predictive control with moving-horizon estimation,” in *Control of Complex Systems*. Elsevier, 2016, pp. 187–209.

- [10] V. Adetola, D. DeHaan, and M. Guay, “Adaptive model predictive control for constrained nonlinear systems,” *Systems & Control Letters*, vol. 58, no. 5, pp. 320–326, 2009.
- [11] A. Mesbah, S. Streif, R. Findeisen, and R. D. Braatz, “Stochastic nonlinear model predictive control with probabilistic constraints,” in *2014 American Control Conference (ACC)*. IEEE, 2014, pp. 2413–2419.
- [12] T. A. N. Heirung, B. E. Ydstie, and B. Foss, “Dual adaptive model predictive control,” *Automatica*, vol. 80, pp. 340–348, 2017.
- [13] H. Fukushima, T.-H. Kim, and T. Sugie, “Adaptive model predictive control for a class of constrained linear systems based on the comparison model,” *Automatica*, vol. 43, no. 2, pp. 301–308, 2007.
- [14] B. Zhu, H. Tazvinga, and X. Xia, “Switched model predictive control for energy dispatching of a photovoltaic-diesel-battery hybrid power system,” *IEEE Transactions on Control Systems Technology*, vol. 23, no. 3, pp. 1229–1236, 2015.
- [15] M. Törchio, N. A. Wolff, D. M. Raimondo, L. Magni, U. Krewer, R. B. Gopaluni, J. A. Paulson, and R. D. Braatz, “Real-time model predictive control for the optimal charging of a lithium-ion battery,” in *2015 American Control Conference (ACC)*. IEEE, 2015, pp. 4536–4541.
- [16] H. H. Abdeltawab and Y. A.-R. I. Mohamed, “Market-oriented energy management of a hybrid wind-battery energy storage system via model predictive control with constraint optimizer,” *IEEE Transactions on Industrial Electronics*, vol. 62, no. 11, pp. 6658–6670, 2015.
- [17] T. A. Nguyen, D. A. Copp, and R. H. Byrne, “Market evaluation of energy storage systems incorporating technology-specific nonlinear models,” *Submitted to IEEE Transactions on Power Systems*, 2018.
- [18] O. Tremblay and L.-A. Dessaint, “Experimental validation of a battery dynamic model for EV applications,” *World Electric Vehicle Journal*, vol. 3, no. 2, pp. 289–298, 2009.
- [19] “<https://www.iso-ne.com/participate/support/web-services-data>,” Online, May 2018.
- [20] J. P. Hespanha, “Tenscalc—a toolbox to generate fast code to solve nonlinear constrained minimizations and compute Nash equilibria,” University of California, Santa Barbara, Tech. Rep., 2017.